AIAA JOURNAL
Vol. 33, No. 11, November 1995

Experimental Research on Blunt Trailing-Edge Airfoil Sections at Low Reynolds Numbers

Junzo Sato* and Yasuto Sunada†
University of Tokyo, Tokyo 113, Japan

The wind-tunnel test results of five airfoil sections with 28.57% chord thickness at chord Reynolds number of 33,000, 66,000, and 99,000 are presented. Lift and drag forces have been measured and flow visualizations have been made. It is shown by cutting off the trailing edge of the section and by making its trailing edge blunt at low Reynolds numbers that the total drag can be reduced, the maximum lift increased, the linearity of lift curve with incidences improved, and the maximum lift-to-drag ratio increased. The structural merits of blunt trailing-edge sections are also discussed.

Nomenclature

C = chord length, 84 mm
C_D = drag coefficient
C_L = lift coefficient
C_{vir} = chord length of the original section
Re = chord Reynolds number, UC/ν
t = maximum thickness, 24 mm
U = wind-tunnel freestream velocity
α = angle of attack, deg

Subscript

vir = original section

Introduction

THE airfoil section characteristics of model airplanes at low Reynolds numbers was studied by Schmitz.[1,2] He found a critical Reynolds number below which the lift decreases and the drag increases almost discontinuously from the conventional values at high Reynolds numbers. The proposed critical Reynolds number for a N60 profile with the 12.41% thickness-to-chord ratio is about 63,000 based on the chord length.[1,2] Similar sudden performance degradation of airfoil sections at low Reynolds numbers has been reported recently.[3–8] Most of the observed characteristics are now attributed[3,4] to the laminar separation of the boundary layer. At low Reynolds numbers, the boundary layer on the surface of airfoils remains laminar over an extensive region, and this separates in the pressure recovery region before the boundary layer becoming turbulent. The separated shear layer frequently reattaches to the surface forming separation bubbles and changing the effective section shapes. At high angles of attack, the bubble bursts and the airfoil stalls, but the bursting of bubbles depends on the history of angle-of-attack change and frequently results in a large hysteresis in the lift vs angle-of-attack curves.

Nagamatsu and Cuche[5] showed the relatively minor supercritical Reynolds number effect on a NACA 63-208 airfoil section over a Reynolds number range of 35,400–176,500. Mueller and Batill[6] showed a very large subcritical effect on a NACA 66_3-018 section at a Reynolds number range of 40,000–400,000. This difference comes mainly from the difference of the thickness-to-chord ratio of the sections they tested. The thinner the section is, the smaller the critical Reynolds number will be. The small leading-edge radius associated with the thinner section creates sharper and higher leading-edge suction peaks at angles of attack, and these sharp pressure suction peaks are effective to promote the laminar to turbulent transition of the separated shear layer, which results in the earlier reattachment of the separation bubbles and reduction of the low Reynolds number effects.

The main object of the present research is to find the basic design principle of the airfoil section profile which effectively shifts Schmitz's critical Reynolds number to lower values. The section must have sufficient thickness in order to secure strength and stiffness of the structures that use the profile. In the usual case of a thick section at low Reynolds numbers, the boundary layer separates just after the maximum thickness, and the section rear-half is covered by laminar separation bubbles. This makes the airfoil wake very thick and increases the drag. Also, the lift cannot increase with an angle of attack because of the large separation bubble. Since the rear-half is covered by the separated flow, there will not be an appreciable difference aerodynamically even if the section is truncated by cutting off the trailing-edge region. If the section chord is truncated, the thickness-to-chord ratio will be increased and the thick section with small leading-edge radius can be obtained. In this paper the blunt trailing-edge airfoil sections are shown to have, at low Reynolds numbers, several more favorable characteristics than the sections with sharp trailing edges.

The intended immediate application of the present research was to use the profile for a streamlined support strut which needs low drag and large thickness-to-chord ratio. The operating Reynolds number range is from several tens of thousands to hundred of thousands. These kinds of sections can have many applications including high-altitude remotely piloted vehicles, model airplanes, propeller sections for human powered aircrafts, sail masts of yachts, high-speed train pantograph members, etc.

Historically well-known research on blunt trailing-edge airfoil sections at a slightly higher Reynolds number of 4×10^5 has been reported by Prandtl and Betz.[9] Many other papers on low Reynolds number airfoil sections have been published recently,[10–14] however, most of them are for the Reynolds number range of 10^5–10^6.

Description of the Experiment

Wind Tunnel

The wind tunnel has a two-dimensional closed wall test section with a 300 mm width by 1200 mm height. The maximum attainable wind speed is 28 m/s. The freestream turbulence intensity is about 0.09% at 5 ~ 6 m/s and 0.13% at 10 ~ 20 m/s. The wind speeds of 6, 12, and 18 m/s were used, and these correspond to the chord Reynolds number Re of 33,000, 66,000, and 99,000, respectively.

Models

The airfoil section models are made of wood and span the tunnel test section. Five models have been tested, and all models have the same chord length of 84 mm and the same maximum thickness

Received Aug. 28, 1994; revision received March 13, 1995; accepted for publication March 16, 1995.

*Professor, Department of Aeronautics and Astronautics, Faculty of Engineering, 7-3-1 Hongo, Bunkyoku. Senior Member AIAA.

†Assistant, Department of Aeronautics and Astronautics, Faculty of Engineering, 7-3-1 Hongo, Bunkyoku.

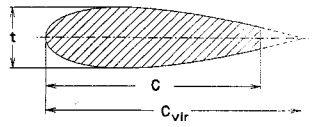

Fig. 1 Construction of the blunt trailing-edge airfoil sections from the NACA 0028.57 section.

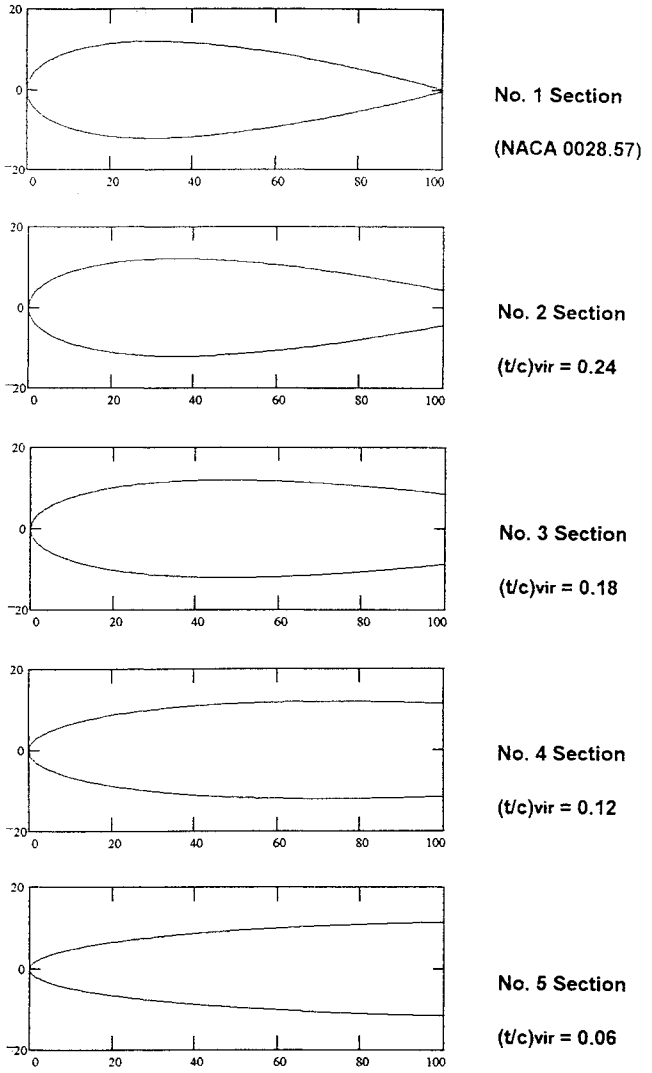

Fig. 2 Five model sections.

of 24 mm. The maximum thickness-to-chord ratio, therefore, is 24/84 = 0.2857 for all models. The NACA four-digit series airfoil section thickness distribution[15] is used to get a section with virtual chord length of C_{vir} and thickness of $t = 24$ mm. The chord length of this section is truncated to $C = 84$ mm by cutting off the section rear end (Fig. 1); thereby a section with a blunt trailing edge is obtained. Figure 2 shows five model section profiles. The virtual thickness-to-chord ratios of sections 1–5 are $(t/C)_{vir} = 0.2857$, 0.24, 0.18, 0.12, and 0.06, respectively. To study the effect of roughness, several tests were also made with added roughness from about 0.1-mm-diam glass spheres distributed thinly around the model leading edges.

Instrumentation and Flow Visualization

The model was supported by a pair of strain-gauge balances that were fixed on the tunnel outside walls. Each balance has two elements to measure lift and drag forces. Small gaps of about 0.5 mm were provided between the model ends and the tunnel inside walls. The balance outputs were low-pass filtered to remove the periodic components, and the tunnel-wall-effect corrections[16] were applied before processing to get lift and drag coefficients. The estimated overall accuracy of the coefficients is, at most, ±2% error for the highest Reynolds number and, at most, ±5% for the lowest number.

To visualize the flowfield, lines of smoke were made by heating the liquid paraffin with a hot wire suspended upstream of the models. Some automobile grease was added to the liquid paraffin in order to increase the viscosity, and this thickened the smoke and prevented the paraffin from dripping down along the heating wire during the measurements.

Results and Discussion

Figures 3, 4, and 5 show the lift and drag coefficients at Re = 33,000, 66,000, and 99,000, respectively. The airfoil section with the sharp trailing edge (section 1) shows very high nonlinearities in the C_L vs α curves, but as the bluntness of the section trailing edge increases, the nonlinearity decreases. At the lowest Reynolds number of 33,000 section 1 can hardly develop any lift through angle-of-attack changes, but section 5 shows almost conventional linear C_L vs α characteristics up to stall angles. A small but almost discontinuous lift increase with incidences observed for sections 3 or 4 at an angle of attack of around 7 deg arises from a discontinuous change of the upper-surface long bubbles into short ones. This phenomenon has also been reported in Refs. 6 and 7. The application of leading-edge roughness is effective only for section 1 to simulate the higher Reynolds number, and the stall angles of attack are increased, but the effect vanishes at $Re = 33{,}000$. At $Re = 66{,}000$ and 99,000, all of the sections except section 5 show some hysteresis in their stall angles of attack. The stall angle obtained by increasing the angle of attack is larger than the angle of attack at which recovery from stall is observed when the incidence is decreased. The amount of hysteresis is reduced as the trailing edge becomes

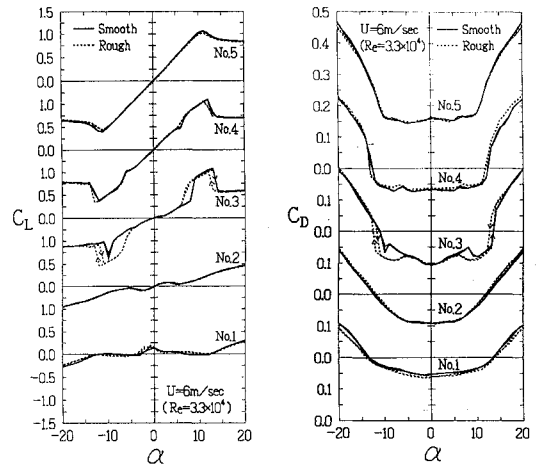

Fig. 3 Experimental results at Re = 33,000: a) C_L vs α and b) C_D vs α.

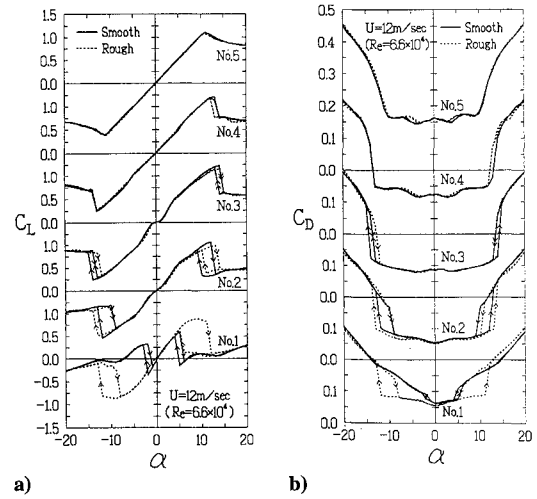

Fig. 4 Experimental results at Re = 66,000: a) C_L vs α and b) C_D vs α.

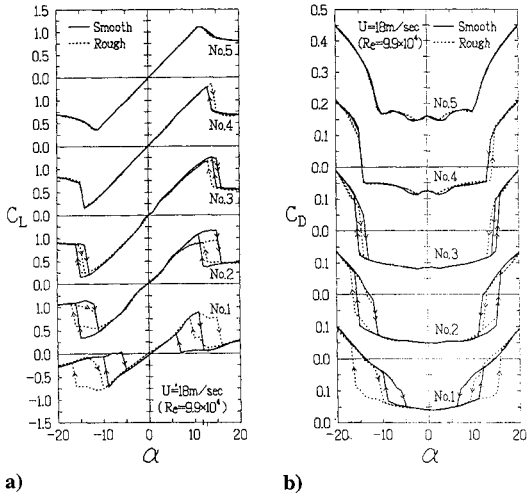

Fig. 5 Experimental results at Re = 99,000: a) C_L vs α and b) C_D vs α.

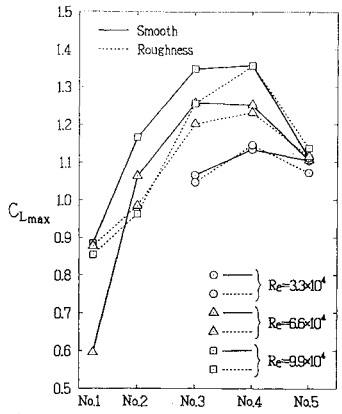

Fig. 6 Comparison of the maximum lift coefficients.

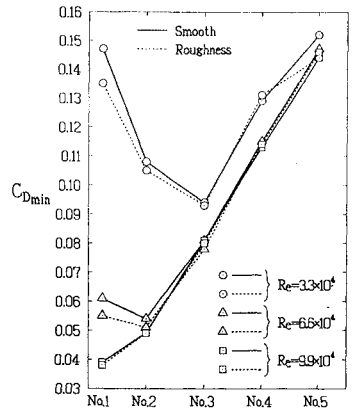

Fig. 7 Comparison of the minimum drag coefficients.

more blunt. Although it is not recorded in the present experiment, the observed periodic oscillations associated with vortex shedding may be effective to reduce the hysteresis.

Figure 6 shows the maximum lift coefficients $C_{L,\max}$ of five sections, and the highest $C_{L,\max}$ is obtained by section 3 or section 4 at all test Reynolds numbers. The $C_{L,\max}$ of section 5 is hardly affected by the test Reynolds number or the leading-edge roughness. The effect of Reynolds number is greatest on the section with the sharp trailing edge, section 1.

The minimum drag coefficients $C_{D,\min}$ are plotted in Fig. 7. At Re = 33,000 section 3 has the lowest $C_{D,\min}$ among the five sections, and at Re = 66,000 section 2 has the lowest. Only at the highest test Reynolds number of 99,000, the section with the sharp trailing edge (section 1) shows the least drag. The minimum drag is not affected much by roughness.

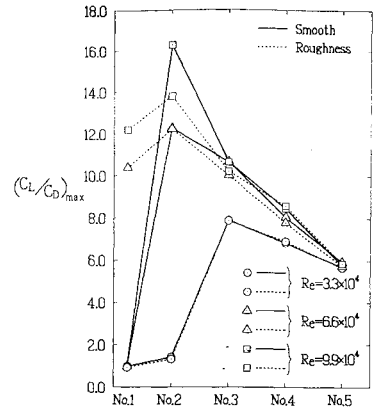

Fig. 8 Comparison of the maximum lift-to-drag ratios.

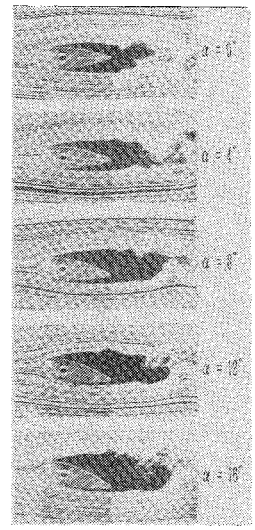

Fig. 9 Flow visualization of the section 1 at Re = 33,000 without roughness.

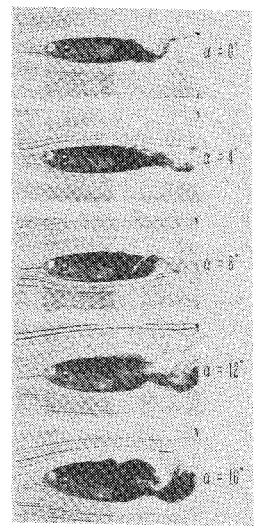

Fig. 10 Flow visualization of section 2 at Re = 33,000 without roughness.

Figure 8 shows the maximum lift-to-drag ratios. At Re = 33,000 section 3 has the highest $(C_L/C_D)_{\max}$, whereas, at higher Reynolds numbers, section 2 does. Roughness can increase the lift-to-drag ratio only for section 1 at Re = 66,000 and 99,000.

Figures 9–13 show flow-visualization pictures of the sections 1–5, respectively. Since the roughness did not show any large effects, flow visualization was conducted only for airfoils without roughness. The most interesting cases of the lowest Reynolds number, Re = 33,000, are presented here. The large separated dead-air

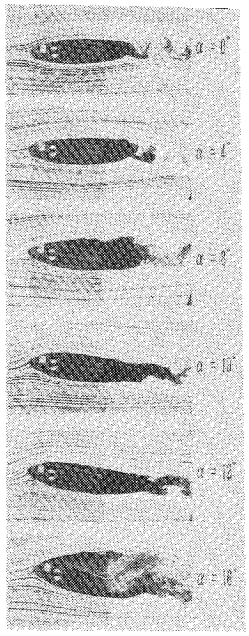

Fig. 11 Flow visualization of section 3 at Re = 33,000 without roughness.

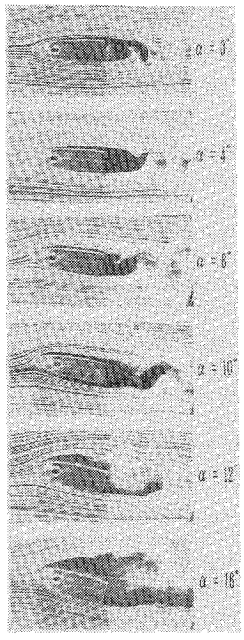

Fig. 12 Flow visualization of section 4 at Re = 33,000 without roughness.

regions, which start from around the maximum thickness and extend into the wake, cover the rear part of section 1 (Fig. 9) and this is the reason for not developing any lift with incidences (Fig. 3a). Only above 12-deg incidences, can further increase of the angle of attack change the outer-flow streamlines. Similar but smaller separated regions are observed for section 2 (Fig 10). In Fig. 11 the laminar separated flow observed on the upper surface of section 3 suddenly disappears at $\alpha = 10$ deg and the upper-surface flow becomes attached, which corresponds to the abrupt small lift increase with increasing incidence shown in Fig. 3a. All of these changes result from the buildup of the leading-edge suction peaks with increasing angle of attack and raising the local Reynolds number. The high local Reynolds number promotes the separated shear layer transition and makes the long bubble corrupt into the short one. At higher angles of attack ($\alpha = 16$ deg), this short bubble bursts and flow separates again from the upper surface.

The virtual section maximum thickness-to-chord ratio decreases as the trailing-edge bluntness increases (cf., Fig. 2). Section 5 has

Fig. 13 Flow visualization of section 5 at Re = 33,000 without roughness.

only a 6% compared to the 28.57% thickness-to-chord ratio of section 1. Although the rear parts are truncated, the leading-edge geometry with smaller leading-edge radius of the thin airfoil is effective in making the leading-edge suction peaks higher and sharper even at small incidences; this prevents the premature formation of long bubbles on the upper surface of sections 4 and 5 and the flow remains essentially attached up to $\alpha = 10$ deg, although the presence of short bubbles is evident in Figs. 12 and 13. At $\alpha = 12$ deg the short bubbles burst, and the long bubbles, typical for thin airfoils at high Reynolds numbers, are formed.

Conclusions

If an airfoil section with a large thickness-to-chord ratio is required at the low Reynolds number of several tens of thousands, it is more favorable to use blunt trailing edges than to use conventional sharp trailing edges. This is effective in preventing the premature formation of large laminar separation bubbles covering most of the airfoil rear surfaces. By adopting the blunt trailing edge to airfoil sections at low Reynolds numbers, the total drag can be reduced despite the associated base-drag penalties, the maximum lift is increased, the linearity of the lift curves with incidences is improved, and the maximum lift-to-drag ratio can be increased. It is also easy to make the section structurally stronger and more rigid by admitting thickness at the trailing edges.

References

[1]Schmitz, F. W., *Aerodynamik des Flugmodells, Tragflugelmessungen I*, Carl Lange Verlag, Duisburg, Germany, 1952, pp. 23, 24, 94–98.

[2]Schmitz, F. W., "Zur Aerodynamik der Kleinen Reynolds-Zahlen," *Jahrbuch 1953 der Wissenschaftlichen Gesellschaft fur Luftfahrt E.V. (WGL)*, Friedr. Vieweg and Sohn, Braunschweig, Germany, 1953, pp. 149–166.

[3]Lissaman, P. B. S., "Low-Reynolds-Number Airfoils," *Annual Review of Fluid Mechanics*, Vol. 15, 1983, pp. 223–239.

[4]McMasters, J. H., and Henderson, M. L., "Low-Speed Single Element Airfoil Synthesis," *Science and Technology of Low Speed and Motorless Flight*, NASA CP2085, Pt. 1, 1979, pp. 1–31.

[5]Nagamatsu, H. T., and Cuche, D. E., "Low Reynolds Number Aerodynamic Characteristics of Low-Drag NACA 63-208 Airfoil," *Journal of Aircraft*, Vol. 18, No. 10, 1981, pp. 833–837.

[6]Mueller, T. J., and Batill, S. M., "Experimental Studies of Separation on a Two-Dimensional Airfoil at Low Reynolds Numbers," *AIAA Journal*, Vol. 20, No. 4, 1982, pp. 457–463.

[7]Pohlen, L. J., and Mueller, T. J., "Boundary Layer Characteristics of the Miley Airfoil at Low Reynolds Numbers," *Journal of Aircraft*, Vol. 21, No. 9, 1984, pp. 658–664.

[8]Mueller, T. J., "The Influence of Laminar Separation and Transition on Low Reynolds Number Airfoil Hysteresis," *Journal of Aircraft*, Vol. 22, No. 9, 1985, pp. 763–770.

[9]Prandtl, P. L., and Betz, P. A., "Messungen an Profilen mit abgeschnittener Hinterkante," *Ergebnisse der Aerodynamischen Versuchsnanstalt zu Gottingen*, Vol. 3, von R. Oldenburg, Berlin, Germany, 1927, pp. 82–85.

[10]Render, P. M., Stollery, J. L., and Williams, B. R., "Aerofoils at Low Reynolds Numbers—Prediction and Experiment," *Proceedings of a Symposium on Numerical and Physical Aspect of Aerodynamic Flows III* (Long Beach, CA), edited by T. Cebeci, Springer–Verlag, New York, 1986, pp. 155–167.

[11]Stollery, J. L., and Dyer, D. J., "Wing-Section Effects on the Flight Performance of a Remotely Piloted Vehicle," *Journal of Aircraft*, Vol. 26, No. 10, 1989, pp. 932–938.

[12]Mueller, T. J. (ed.), "Low Reynolds Number Aerodynamics," Proceedings of the Conference (Notre Dame, IN), *Lecture Notes in Engineering*, edited by T. J. Mueller, Vol. 54, Springer–Verlag, New York, 1989, pp. 1–230.

[13]Cebeci, T., "Essential Ingredients of a Method for Low Reynolds-Number Airfoils," *AIAA Journal*, Vol. 27, No. 12, 1989, pp. 1680–1688.

[14]Pfenninger, W., and Vemuru, C. S., "Design of Low Reynolds Number Airfoils, Part I," *Journal of Aircraft*, Vol. 27, No. 3, 1990, pp. 204–210.

[15]Abbott, I. H., and von Doenhoff, A. E., "Theory of Wing Sections," Dover, New York, 1959, p. 113.

[16]Allen, H. J., and Vincenti, W. G., "Wall Interference in a Two-Dimensional-Flow Wind Tunnel, with Consideration of the Effect of Compressibility," NACA Rept. 782, 1944.